Astro 735: Cosmology
Lecture 3: Galaxies and Quasars

Elena D'Onghia

1 Aside: Magnitudes

Astronomers often measure luminosities on an inverse logarithmic scale of "absolute magnitude:"

$$M = -2.5 \log L + \text{ constant}, \tag{1}$$

where the luminosity of the Sun is usually used for the normalization. It also depends on the band (wavelength range) in which the object is observed. For an object of luminosity L_C in band C, the absolute magnitude M_C is

$$M_C = -2.5 \log(L_C/L_{C\odot}) + M_{C\odot}, \tag{2}$$

where $L_{C\odot}$ and $M_{C\odot}$ are the luminosity and absolute magnitude of the Sun in band C.

We also measure "apparent magnitudes," which are a measurement of the apparent rather than the intrinsic brightness of an object. In wavelength band C, for an object with observed flux F_C,

$$m_C \equiv C = -2.5 \log F_C + \alpha_C, \tag{3}$$

where α_C is a constant which is chosen such that, in the absence of absorption, the apparent magnitude m_C is equal to the absolute magnitude M_C if the object is at a distance of 10 pc. The difference between the absolute magnitude and the apparent magnitude is called the distance modulus, since if we know both magnitudes we can then determine how far away the object is.

Note that that M can refer to either absolute magnitude or mass, so pay attention to context.

2 Galaxies

Galaxies are gravitationally bound clusters of stars, gas and dark matter. Galaxies have a variety of morphologies (generally divided into spiral, elliptical and irregular, with the proportion of irregular galaxies strongly increasing with increasing redshift), sizes and masses. Most of the light in the universe is produced in galaxies containing 10^{10}–10^{11} stars that generate a typical galactic luminosity of $\langle L_{\rm gal}\rangle \sim 2 \times 10^{10}$ $\mathrm{L}_\odot$.

2.1 Components of a galaxy

The major components of a typical spiral galaxy such as the Milky Way are shown in Figure 1. The visible portion of the galaxy is entirely contained in the disk and bulge, but most of the mass is in the dark matter halo.

Elliptical galaxies have a triaxial ellipsoid of stars similar to the bulge of a spiral galaxy within a much larger dark halo.

A useful quantity to describe galaxies or galaxy clusters is the mass-to-light ratio, the ratio of the mass of the galaxy in solar units to its luminosity in solar units. The visible part of a typical galaxy has a typical visible mass-to-light ratio $\langle M_{\rm vis}/L\rangle \sim 3$ ($\mathrm{M}_\odot/\mathrm{L}_\odot$; the units are usually omitted). This depends on the types of stars in the galaxy; massive stars have much lower mass-to-light ratios than low mass stars, as is apparent from the stellar mass-luminosity relation.

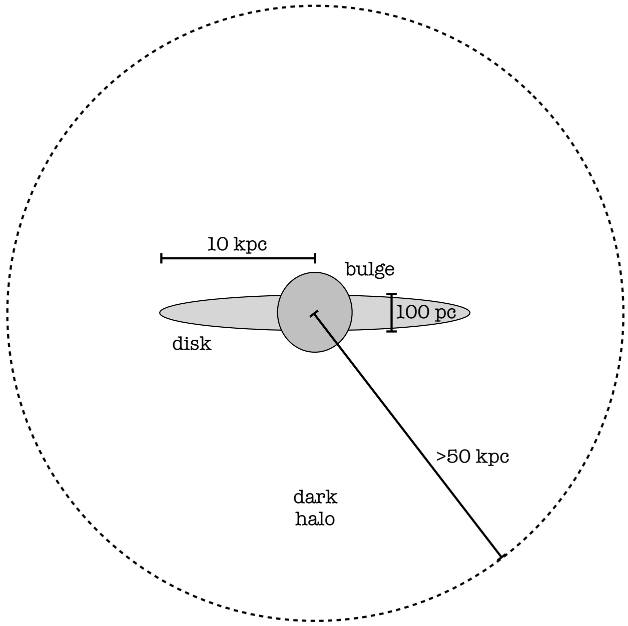

Figure 1: Schematic diagram of the major components of a typical spiral galaxy.

2.2 Rotation curves and dark matter halos

For cosmological purposes we are most interested in dark matter and the total masses of galaxies. Looking at the stars in galaxies tells us about the distribution of luminous matter, but not about the total distribution of mass. Measurements of total masses of galaxies come from kinematic studies. For spiral galaxies, we measure the **rotation curve**: the rotational velocity as a function of radius. A typical rotation curve is shown in Figure 2 (data points). Rotational velocities are usually measured from the Doppler shift of the 21-cm hyperfine transition of neutral hydrogen. Note that it is flat at 150 km s^{-1} to the largest radius we can measure. Also shown are the gravitational contributions of stars and gas to the rotation. The rotation curve of the Milky Way flattens at about 220 km s^{-1}.

This has important implications for the mass distribution of galaxies. Setting the gravitational and centripetal forces equal (for a particle of mass m, in a circular orbit at radius r around a spherically symmetric mass distribution M):

$$v_c^2 = \frac{GM}{r}. \tag{4}$$

and

$$\frac{dM}{dr} = \frac{v_c^2}{G}. \tag{5}$$

Since v_c is constant, $M(r) \propto r$. Because the mass keeps increasing as far out as we can measure, we can only place a lower limit on the total galactic mass and mass-to-light ratio. For the example in Figure 2, $M/L > 20\ h_{70}$ (the factor of H_{70} comes from the use of Hubble's law to convert angular size to physical size).

The density profile of dark matter halos is often described with the "NFW profile" (Navarro, Frenk and White), based on cosmological simulations of galaxy formation:

$$\rho(r) \propto \frac{1}{r(1 + r/r_s)^2}, \tag{6}$$

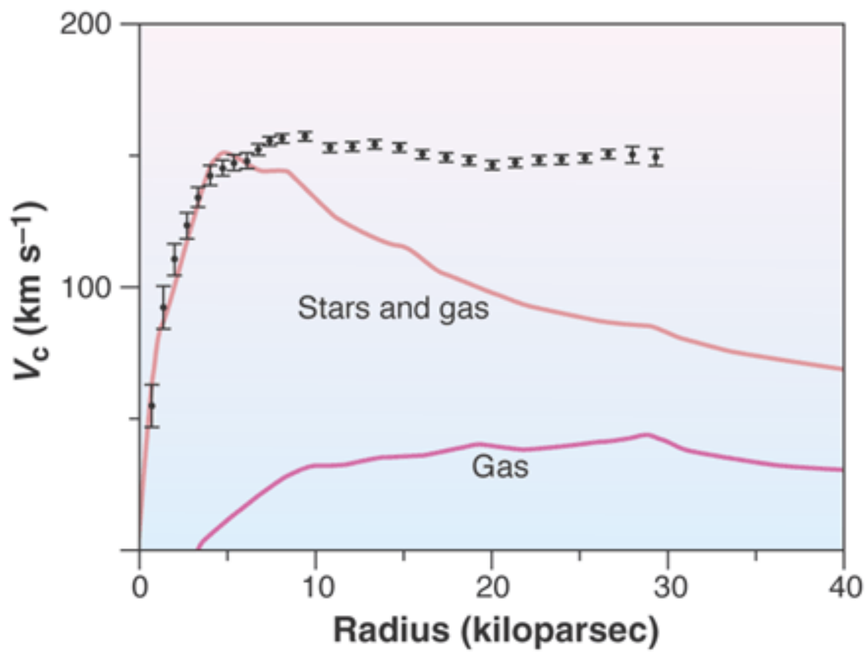

Figure 2: The data points show the rotation curve of NGC 3198, a typical spiral galaxy. The solid lines show the predicted rotation curve based on the observed distributions of stars and gas (Freeman 2003, *Science*, 302, 1902).

where r_s parameterizes the size of the halo. The density falls as r^{-3} for $r \gg r_s$, so the integrated mass rises logarithmically with r and the total halo mass is undefined. In practice the halo mass is defined as the mass within the radius where objects are bound. We'll see later from the theory of structure formation that the mean density within this radius is ~ 200 times the mean universal density.

The simple rotation curve analysis above shows that $\rho(r) \propto r^{-2}$, which is a reasonable first approximation to the halo density profile. This is called an **isothermal sphere**, and can be written as

$$G\rho(r) = \frac{\sigma_v^2}{2\pi r^2}, \tag{7}$$

where σ_v is the one-dimensional velocity dispersion of objects bound in the potential. This has a radial dependence intermediate between the large and small r dependencies of the NFW profile, so it's a reasonable approximation over a large range of r.

2.3 The luminosity function

The approximate number density of bright galaxies is $n_{\rm gal} \sim 0.015$ Mpc^{-3}, which corresponds to a typical intergalactic distance of ~ 4 Mpc. This refers to *bright* galaxies; the total number of galaxies is ill-defined because of the difficulty in detecting the large numbers of faint galaxies. The total light output of the universe comes mostly from bright galaxies, and is

$$J \sim \langle L_{\rm gal}\rangle n_{\rm gal} \sim 10^8 \ {\rm L_\odot \ Mpc^{-3}} \tag{8}$$

The total mass density associated with the visible parts of galaxies is then

$$\rho_{\rm vis} = J\langle M/L\rangle \sim 3\times 10^8 \ {\rm M_\odot \ Mpc^{-3}}. \tag{9}$$

We use large galaxy surveys (redshift surveys, since galaxy redshifts are what we actually measure is galaxy redshifts) to measure the number of galaxies per unit volume and per unit luminosity interval. This is called the **luminosity function**, and is usually parameterized by the "Schechter function:"

$$\frac{dN_{\rm gal}}{dV\,dL} = \frac{\phi_*}{L_*}\left(\frac{L_*}{L}\right)^{\alpha} \exp(-L/L_*), \tag{10}$$

where ϕ_*, L_* and α are constants with $\alpha \sim 1$. L_* is a characteristic galaxy luminosity, ϕ_* is the density of L_* galaxies, and α is the slope at the faint end of the distribution. An example of the luminosity function, for galaxies at redshifts $z \sim 2$, $z \sim 3$ and $z \sim 4$, is shown in Figure 3 (this figure, and much observational data, uses magnitudes M instead of luminosity). Inspection of this figure and of Equation 10 shows that the number of bright galaxies falls off exponentially, while the number of faint galaxies rises as a power law with slope α. Galaxies of the characteristic luminosity L_* divide the two regimes.

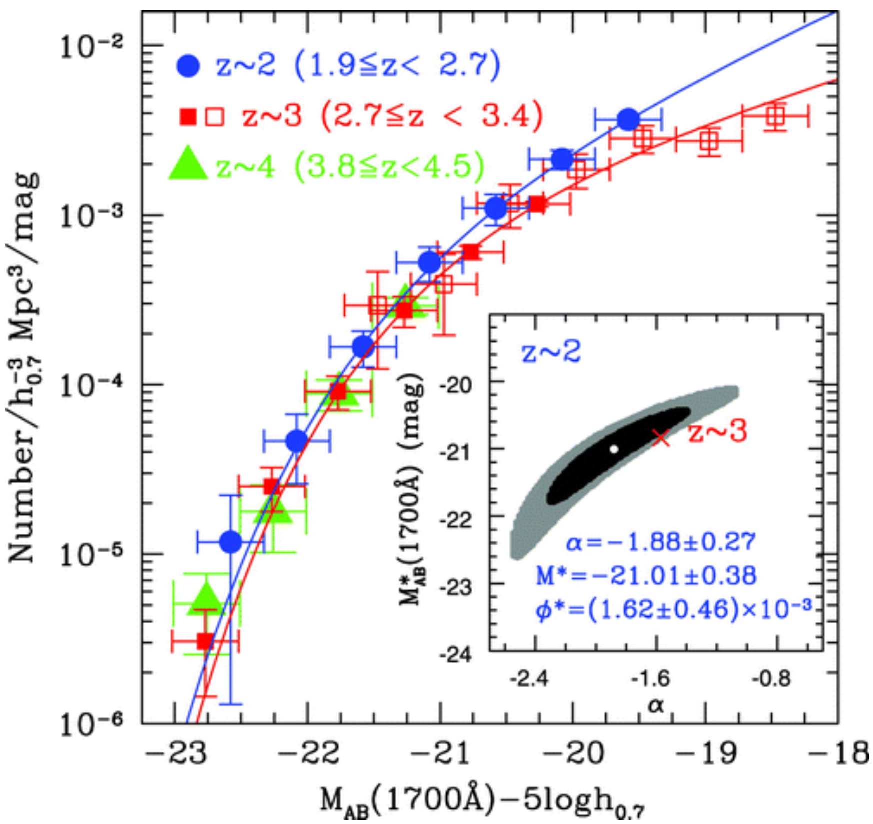

Figure 3: An example of Schechter luminosity functions fit to galaxies at $z \sim 2$, $z \sim 3$ and $z \sim 4$ (Reddy et al 2008, *ApJS*, 175, 48). The x axis plots the absolute galaxy magnitude, which is an inverse logarithmic measurement of luminosity. Bright galaxies are on the left and faint galaxies on the right. (Astute observers may notice that the best-fit value for α in this figure is negative. This is because the term of the Schechter function involving α is often written as $(L/L_*)^{\alpha}$ rather than $(L_*/L)^{\alpha}$ as in Equation 10; this changes the sign of α.)

In the local universe, where galaxy surveys are large and reasonably complete, we have a good measurement of the luminosity function from the Sloan Digital Sky Survey (SDSS) and the Two Degree Field Redshift Survey (2dFRS). From SDSS, for galaxies at $z \sim 0.1$ measured near $\lambda \sim 560$ nm, we have

$$\phi_* = (0.511 \pm 0.016) \times 10^{-2} h_{70}^3 \,\mathrm{Mpc}^{-3} \tag{11}$$

$$\begin{aligned} L_* &= (2.45 \pm 0.02) h_{70}^{-2} \times 10^{10}\ \mathrm{L}_\odot && (12) \\ \alpha &= 1.05 \pm 0.001 && (13) \end{aligned}$$

Also note that the luminosity distribution diverges logarithmically at faint L, making the total number of galaxies ill-defined. However, because faint galaxies produce little light, the total light output per unit volume is finite. If the Schechter function is $\phi(L)$, then the total number of galaxies per unit volume is $n = \int \phi(L) dL$, and the total luminosity density is $J = \int L\phi(L) dL$. We can therefore estimate the total luminosity density for the SDSS survey, where $\alpha = 1$:

$$J = \int_0^\infty dL \phi_* \exp(-L/L_*) \sim L_* \phi_* = 1.29 h_{70} \times 10^8\ \mathrm{L}_\odot\ \mathrm{Mpc}^{-3} \tag{14}$$

Most of the light comes from galaxies brighter than $\sim 10^9\ \mathrm{L}_\odot$, so we can calculate the number density of bright galaxies by integrating the luminosity function over luminosity above that limit:

$$n_{\rm gal} = \int_{10^9}^\infty dL \frac{\phi_*}{L} \exp(-L/L_*) = 0.015 h_{70}^3\ \mathrm{Mpc}^{-3}. \tag{15}$$

3 Quasars

The most luminous objects in the universe are quasars (also called QSOs, for "quasi-stellar" object, since they appear to be star-like point sources in images). These are part of a category of objects called Active Galactic Nuclei (AGN), and are believed to be powered by the accretion of gas onto a supermassive ($M > 10^6\ \mathrm{M}_\odot$) black hole at the center of a galaxy. The release of gravitational potential energy through mass accretion is a very efficient way to generate energy, accounting for the large luminosity of quasars.

Distinctive characteristics of AGN (but not all have all of these features):

- Large amounts of nonstellar emission, some of it nonthermal in origin. Active galaxies produce more X-ray and radio emission than would be produced by their stars.
- Light from AGNs is variable on short timescales, at virtually all wavelengths. Timescale for variability depends on luminosity and wavelength, with most rapid variability seen at short wavelengths and low luminosities. X-rays in low luminosity AGNs can vary on timescales of minutes. The variation timescale places an upper limit on the size of the emitting region, since an object can't vary on a timescale faster than the time it takes for light to cross the object.
- Some active galaxies have jets detectable at X-ray, visible and radio wavelengths. The jets contain ionized gas flowing outward at relativistic speeds
- The UV, visible and IR spectra of AGNs are dominated by strong emission lines.

The fact that most galaxies today contain large central black holes suggests that a quasar phase may be a part of the evolution of most galaxies.

Quasars are important cosmological probes, since they are so bright and can be seen to high redshifts (the highest is currently at $z = 7.1$, 770 Myr after the Big Bang). They place important constraints on structure formation, since it must have proceeded rapidly for such objects to exist at $z \sim 7$.

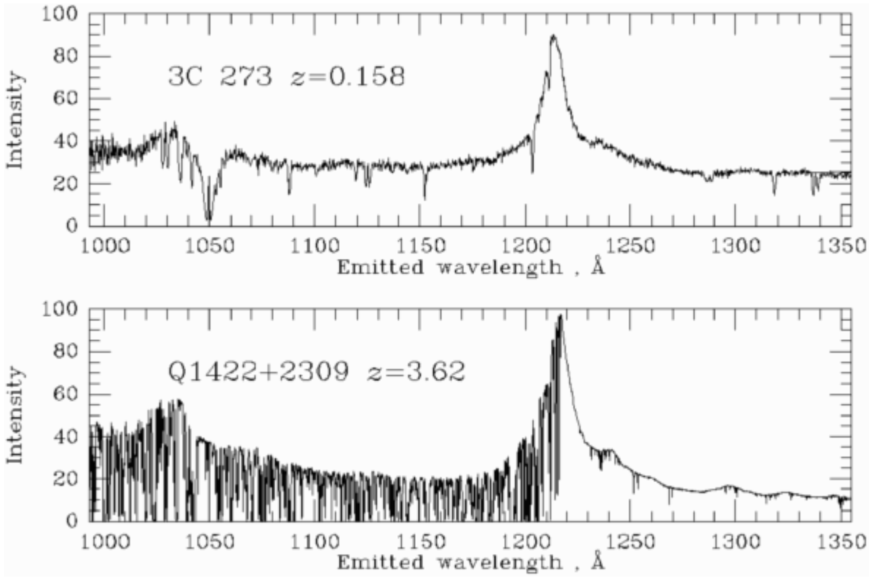

Figure 4: The spectra of a relatively nearby QSO (top panel) and a high redshift QSO (bottom panel). The Lyα forest is visible in the spectrum of the high redshift QSO.

4 The intergalactic medium and the Lyα forest

The second reason that quasars are extremely important cosmological probes is that they allow us to make sensitive measurements of the intergalactic medium. The spectrum of a QSO is dominated by a strong, broad Lyα emission line (Lyα is the $n = 2$ to $n = 1$ transition of hydrogen). Blueward of this emission line, the spectrum shows absorption lines from gas along the line of sight to the quasar.

As photons from the quasar travel toward us, they decrease in energy because of the cosmological redshift. They pass through clouds of gas on the way, and if the energy of the photon is equal to the energy of the Lyα transition in the rest frame of the cloud it will be resonant at Lyα and can be absorbed. The result is a forest of narrow absorption lines in the QSO spectrum blueward of the emission from Lyα in the QSO itself. In the (rest frame) spectrum of the QSO, the lines appear at wavelengths

$$\lambda = \lambda_{\mathrm{Ly}\alpha} \left(\frac{z_{\mathrm{cloud}} + 1}{z_{\mathrm{QSO}} + 1} \right), \tag{16}$$

where $\lambda_{\mathrm{Ly}\alpha} = 1215$ Å (121.5 nm; observational astronomers usually use angstroms) is the wavelength of the Lyα transition. As we would expect, the higher the redshift of the QSO, the more intervening clouds it can pass through, and the more significant the Lyα forest effect. This is shown in Figure 4. We think that most of the baryons in the universe live outside of galaxies, so this is probably the most sensitive probe we have of the mass distribution in the universe. The observed number density of these absorbing clouds places important constraints on the theory of structure formation, and allows us to determine the quantity and chemical state (through absorption lines from elements other than hydrogen) of intervening gas. We will discuss this in more detail when we discuss structure formation.